Electronic Supplementary Information

A near-infrared fluorescent probe for ratiometric sensing of SO_2 in cells and zebrafish

Mengya Lv,[a] Yanhao Zhang,[c] Jiayi Fan,[a] Yanyun Yang,[a] Sheng Chen,[*,a, b] Gaolin Liang,[*, b] and Shusheng, Zhang[*,b]

[a]College of Chemistry, Zhengzhou University, 100 Kexue Road, Zhengzhou, Henan 450001, China

[b]Center for Advanced Analysis & Gene Sequencing, Zhengzhou University, 100 Kexue Road, Zhengzhou, Henan 450001, China

[c]State Key Laboratory of Environmental and Biological Analysis, Department of Chemistry, Hong Kong Baptist University, Hong Kong SAR, China

Table of Contents:

1. Synthesis, ^{1}H- and ^{13}C-NMR, HR-MS

Synthesis of compound 1. The solution of 2-hydroxy-1-naphthaldehyde (516 mg, 3 mmol), acrolein (0.5 mL, 7.5 mmol) and K_2CO_3 (1.035g, 7.5mmol) in 1,4-dioxane (60 mL) was heated at 105 °C for 72 h. After the reaction was completed, it was removed from the heating bath, poured into 150 mL of ice water. The resulting mixture was extracted three times with ethyl ether (40 mL). The combined organic layer was washed with saturated NaCl twice, then dried over anhydrous Na_2SO_4, and concentrated under vacuum. Then, the crude product was purified by column chromatography on silica gel (ethyl acetate: petroleum ether = 1:5, *v/v*) to afford light yellow solids (203 mg, 32.2% yield). ^{1}H NMR (400 MHz, $CDCl_3$) δ (ppm): 9.64 (s, 1 H), 7.96 (d, *J* = 8.4 Hz, 1 H), 7.87 (s, 1 H), 7.79 (d, *J* = 8.9 Hz, 1 H), 7.76 (d, *J* = 8.2 Hz, 1 H), 7.61-7.51 (m, 1 H), 7.46-7.37 (m, 1 H), 7.07 (d, *J* = 8.9 Hz, 1 H), 5.09 (s, 1 H); ^{13}C NMR (101 MHz, $CDCl_3$) δ (ppm): 189.52 (s), 155.82 (s), 137.57 (s), 134.11 (s), 130.64 (s), 129.33 (s),129.29 (s), 128.92 (s), 128.03 (s), 124.58 (s), 120.97 (s), 117.68 (s), 113.89 (s), 63.13 (s). HR-MS (ESI, *m/z*) Calcd for $[M+H]^+$, 211.0714; Found, 211.0771.

Synthesis of compound 2. The solution of 2,3,3-trimethylindolenine (160 mg, 1 mmol) and 1,3-propane sultone (150 mg, 1.2 mmol) in toluene (5 mL) was heated under reflux for 24 h. The resulting solution was cooled to room temperature and filtered. The filtered product was washed with diethyl ether and dried in vacuo to give compound 2 (250 mg, 89% yield) as a pink solid. ^{1}H NMR (400 MHz, DMSO-d_6) δ (ppm): 8.09-8.04 (m, 1 H), 7.85 (dd, *J* = 5.8, 2.8 Hz, 1 H), 7.67-7.56 (m, 2 H), 4.72-4.63 (m, 2 H), 2.86 (s, 3 H), 2.66 (t, *J* = 6.7 Hz, 2 H), 2.18 (p, *J* = 7.1 Hz, 2 H), 1.55 (6 H); ^{13}C NMR (101 MHz, DMSO-d_6) δ (ppm): 197.11 (s), 142.43 (s), 141.67 (s), 129.80 (s), 129.41 (s), 123.95 (s), 115.94 (s), 54.63 (s), 54.36 (s), 47.89 (s), 47.06 (s), 24.21 (s), 22.53 (s), 14.33 (s). HR-MS (ESI, *m/z*) Calcd for $[M+H]^+$, 282.1119; Found, 282.0936.

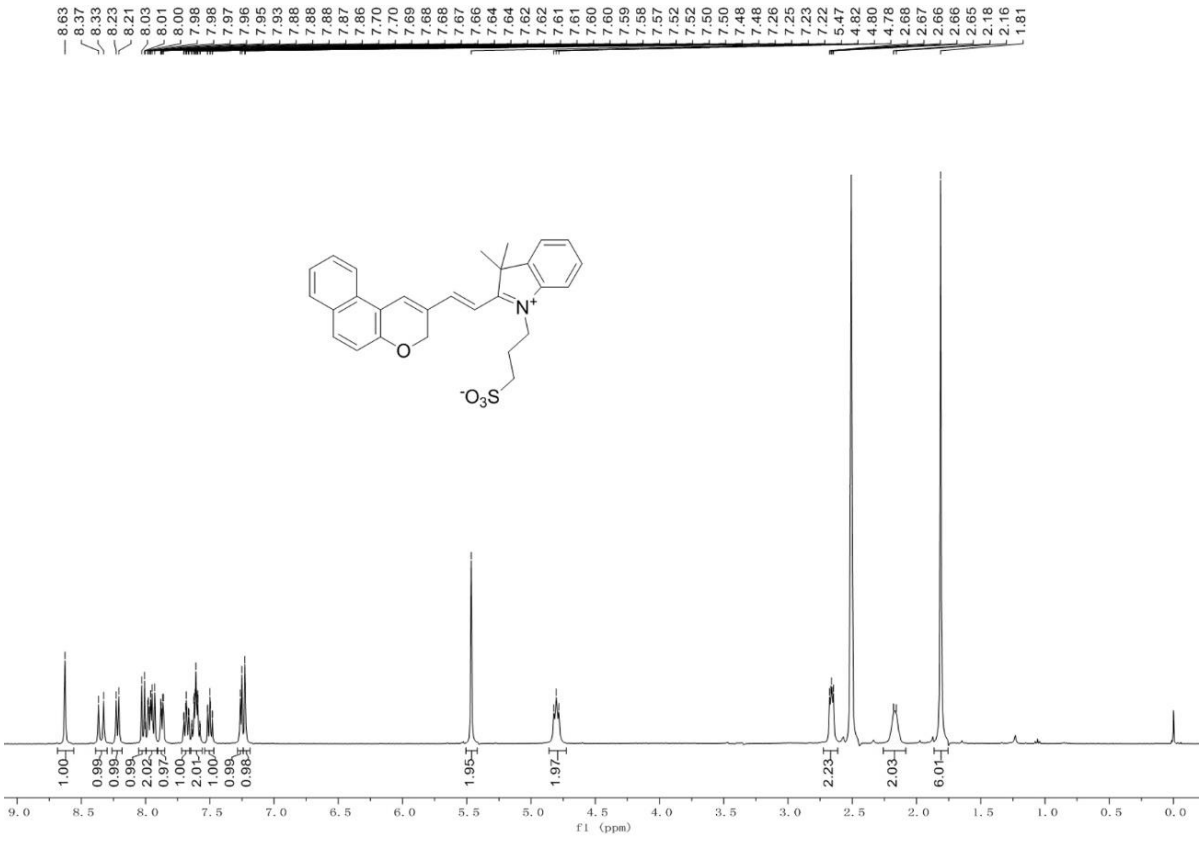

Figure S1. ^{1}H NMR spectrum (DMSO-d_6) of probe **Mito-HN**

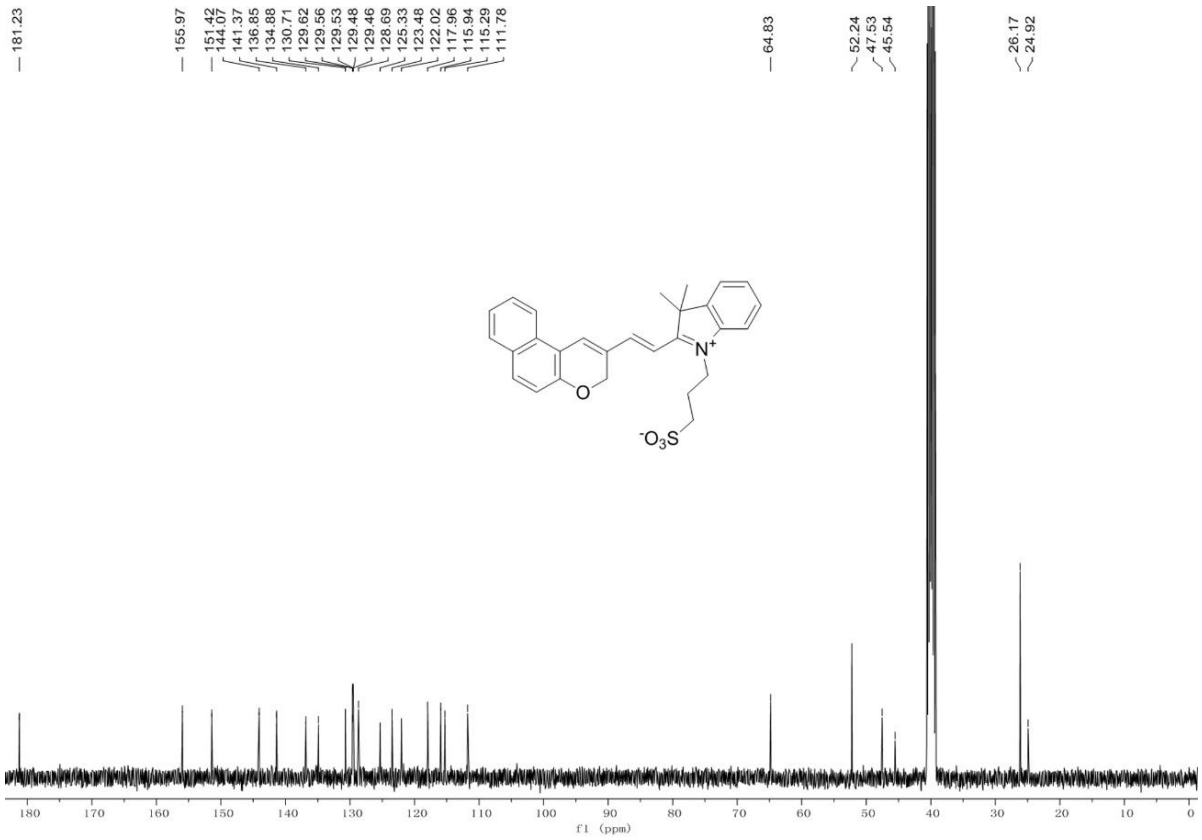

Figure S2. ^{13}C NMR spectrum (DMSO-d_6) of probe **Mito-HN**

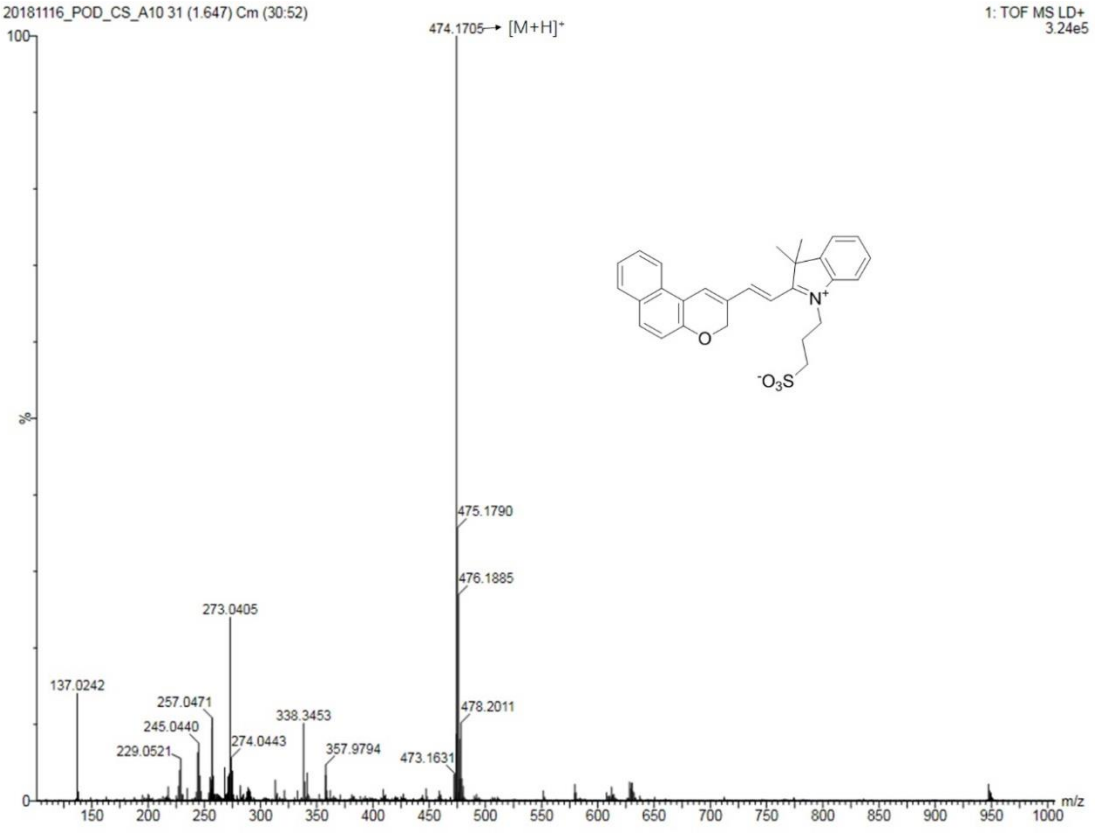

Figure S3. MALDI -MS spectrum of probe **Mito-HN**

2. AIEE mechanism and sensing mechanism.

Table S1. Optical properties of **Mito-HN** before and after reaction with SO_2, **Mito-HN** crystalline powder, **Mito-HN** in water, PBS, and MeOH/glycerol mixtures with different glycerol fractions.

Series	λ_{max} (nm)	ε (M^{-1} cm^{-1})	λ_{em} (nm)	Φ_F[a]	Stokes shift (nm)
Mito-HN in PBS (10% DMSO)	530	2.7×10^4 M^{-1} cm^{-1}	668	3.31%	138
Mito-HN-$NaHSO_3$ in PBS (10% DMSO)	345	1.9×10^4 M^{-1} cm^{-1}	520	2.24%	175
Mito-HN in water	530		668	2.53%	
Mito-HN in PBS	530		668	2.52%	
Mito-HN in CH_3OH	530	\	668	0.72%	\
Mito-HN in CH_3OH/glycerol (5:5)	530	\	668	1.78%	\
Mito-HN in CH_3OH/glycerol (2:8)	530	\	668	4.37%	\
Mito-HN in Crystalline powder	\	\	688	12.05%	\

[a] Fluorescence quantum yield (Φ_F) in solution was determined using rhodamine B (0.89) in ethanol as a standard. Φ_F in the solid state was obtained using an integrating sphere with excitation at 365 nm on an Edinburgh FLS 1000 fluorescence spectrometer.

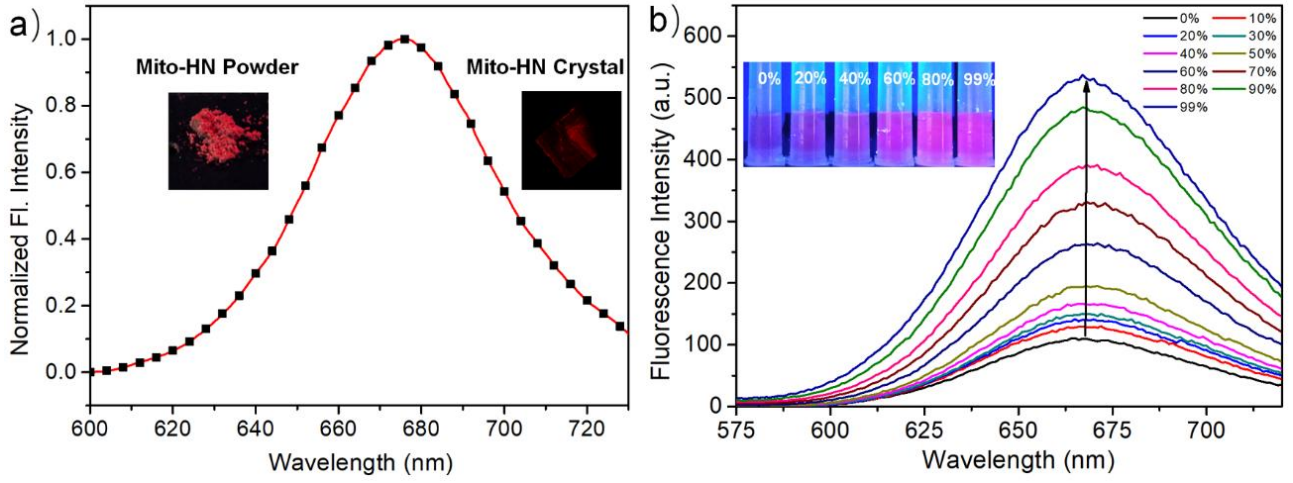

Figure S4. (a) Normalized fluorescence spectra of the solid powders of **Mito-HN**. Inset: photos of as-prepared solid powders and the red crystal of **Mito-HN** under UV light. (b) Fluorescence spectra of **Mito-HN** (10 μM) in MeOH/glycerol mixtures with different glycerol fractions. Inset: photos of **Mito-HN** (10 μM) in MeOH/glycerol mixtures with different glycerol fractions under UV light.

Table S2. Selected crystallographic data for probe **Mito-HN**.

crystals	**Mito-HN**
formula	$C_{28}H_{27}NO_4S$
fw [g·mol^{-1}]	473.58
crystal color	Red
crystal system	Monoclinic
space group	P_{21}/c
a [Å]	7.68126(19)
b [Å]	22.6995(5)
c [Å]	17.9400(3)
α [º]	90
β [º]	95.2798(19)
γ [º]	90
V [Å^3]	3114.76（12）
Z	4
ρ_{calcd} [g/cm^3]	1.372
μ [mm^{-1}]	4.371
T [K]	293
θ_{max} [º]	67.077
R/wR [$I > 2\sigma_{(1)}$]	0.0683/0.2148

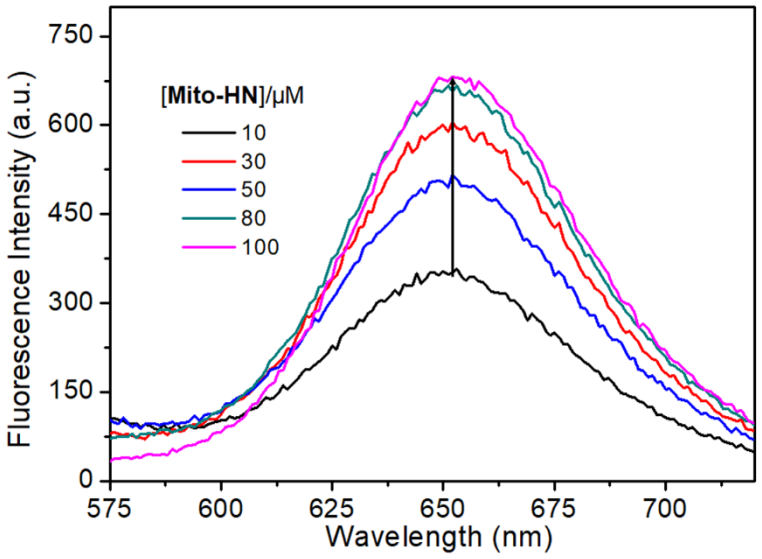

Figure S5. Fluorescence spectra of different concentration of **Mito-HN** (10, 30, 50, 80, 100 μM) in PBS (10 mM, pH 7.4, containing 10% DMSO).

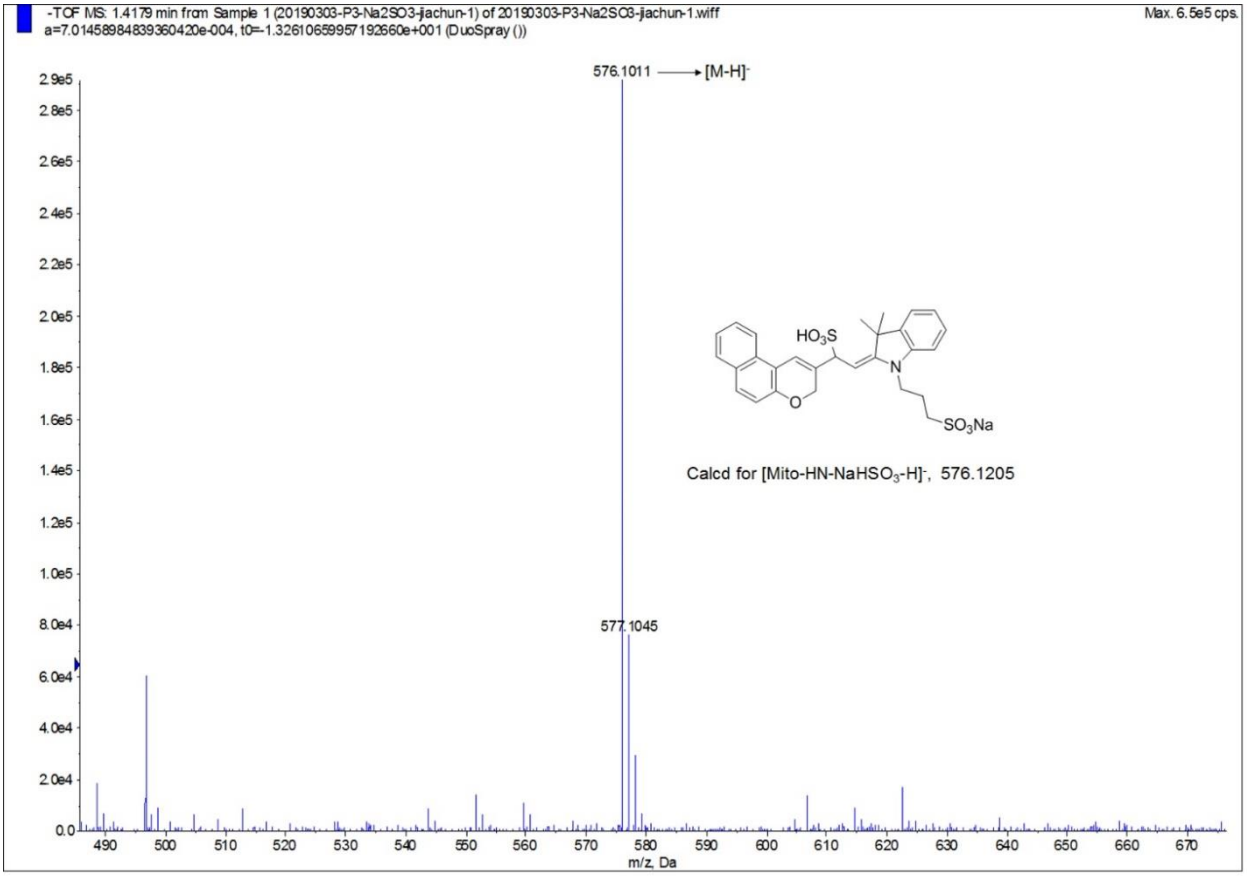

Figure S6. ESI-MS of **Mito-HN** treated with Na_2SO_3 or $NaHSO_3$.

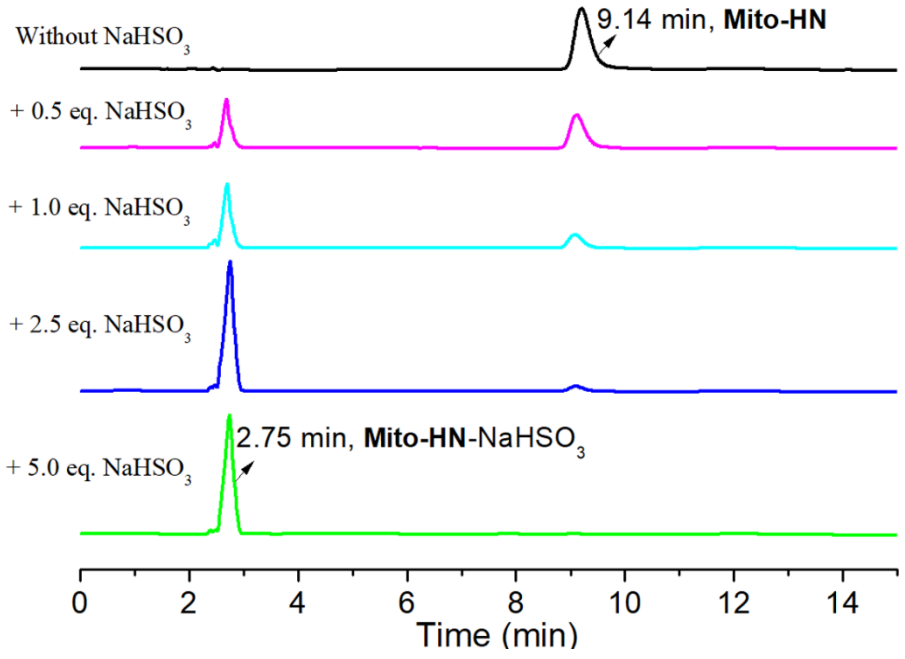

Figure S7. The HPLC chromatograms of **Mito-HN** in the precence of different equivalents of $NaHSO_3$.

3. Sensing properties of probe Mito-HN toward HSO_3^-/SO_3^{2-}.

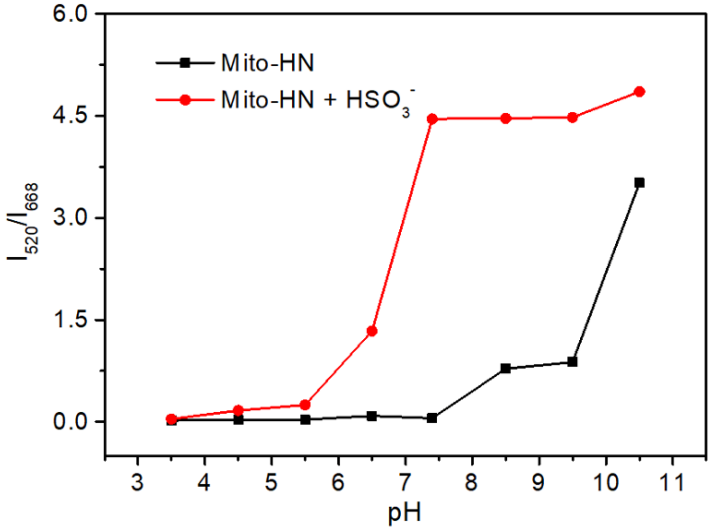

Figure S8. The pH effects on the fluorescence behavior of 10 μM **Mito-HN** (black line) and 10 μM **Mito-HN** with 100 μM HSO_3^- (red line) in PBS (10 mM, containing 10% DMSO).

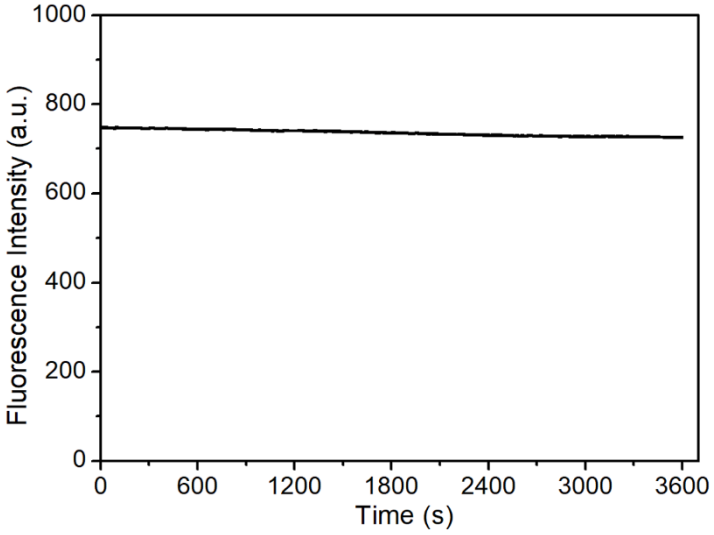

Figure S9. Fluorescence intensity of **Mito-HN** (10 μM) as a function of time in PBS (10 mM, pH 7.4, containing 10% DMSO).

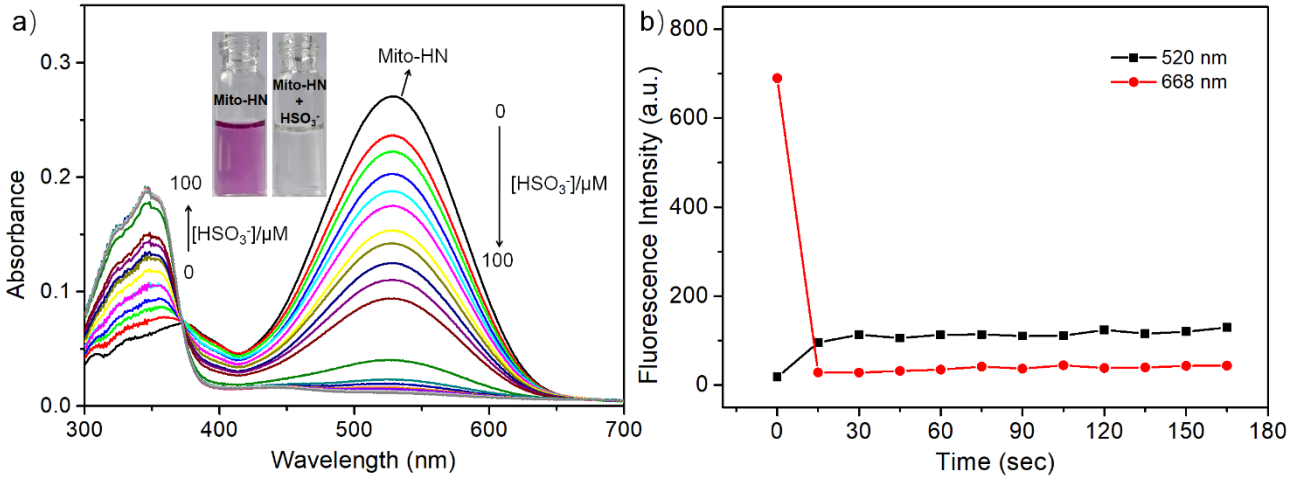

Figure S10. (a) Absorption spectra changes of **Mito-HN** (10 μM) upon addition of HSO_3^- (0-100 μM) in PBS (10 mM, pH 7.4, containing 10% DMSO). (b) Time-dependent fluorescence intensity changes at 520 nm and 668 nm of **Mito-HN** (10 μM) in the presence HSO_3^- (100 μM) in PBS (10 mM, pH 7.4, containing 10% DMSO).

The detection limit was calculated with the following equation:

$$\text{Detection limit} = 3S_b/k$$

Where S_b is the standard deviation of blank measurements, which was achieved by measuring the fluorescence spectrum of probe **Mito-HN** ten times, and k is the slope of the fitted line.

Table S3. Comparison of fluorescent probes for SO_2 dervatives.

Probes	$\lambda_{ex}/\lambda_{em}$ (nm)	Detection medium	Detection limit	Applications	Ref.
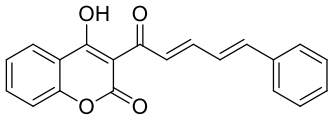	377/450	PBS (10 mM, pH 7.4)	0.01×10^{-6} M	Sugar samples	S1
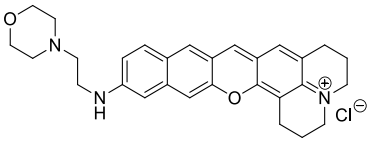	480/512 480/704	PBS (pH 5.0, 30% EtOH, 1% DMSO)	0.09×10^{-6} M	Lysosome-tar geted ,cell	20
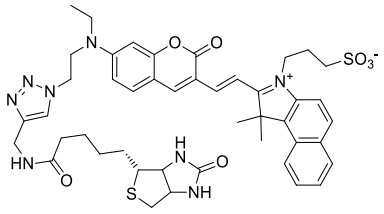	467/505 467/652	PBS (pH 7.4, 10 mM, containing 30% DMF)	0.072×10^{-6} M	Lysosome-tar geted, cell	21

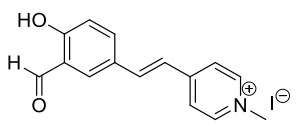	460/550	PBS (pH 7.4, containing 90% DMSO)	0.0131 × 10^{-6} M	Cell and zebrafish	22
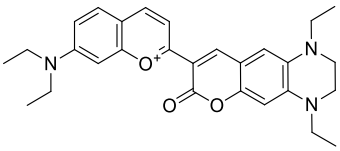	466/585	HEPES buffer (pH = 7.4)	0.0083 × 10^{-6} M	Cell	37
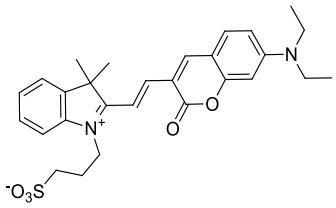	450/485 450/667	PBS (20 mM, pH 7.4, containing 50% MeOH)	0.027 × 10^{-6} M	Sugar samples, cell	30
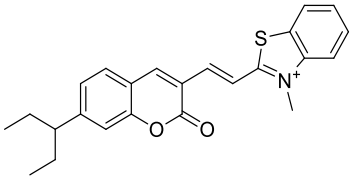	410/478	PBS (10 mM, pH 7.4, containing 30% DMF)	0.38 × 10^{-6} M	Cell	S2
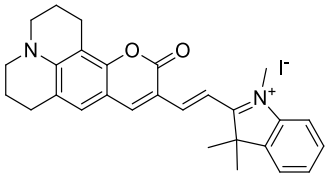	470/515 470/681	PBS (20 mM, pH 7.4, containing 0.4% DMSO)	0.53 × 10^{-6} M	Mitochondria -targeted, cell	S3
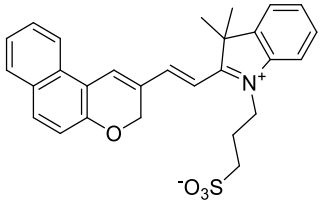	375/520 375/668	PBS (10 mM, pH 7.4, 10% DMSO	0.17× 10^{-6} M	Mitochondria -targeted, cell and zebrafish, AIEE	This work

4. Selectivity and interference.

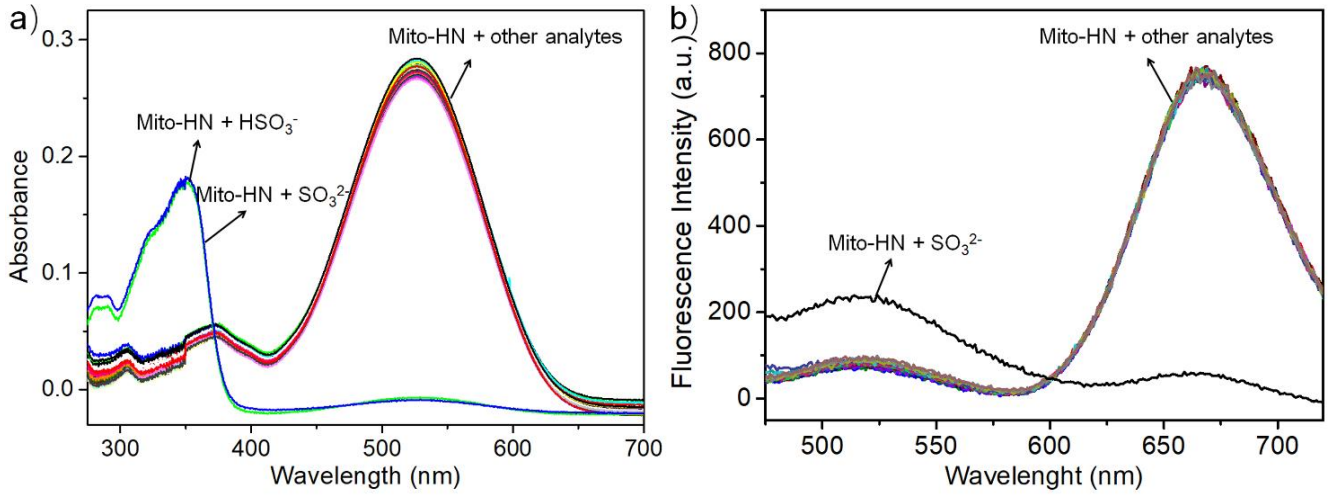

Figure S11. (a) Absorption spectra of **Mito-HN** (10 μM) in the presence of various species, including SO_3^{2-}, HSO_3^-, Ca^{2+}, Al^{3+}, Zn^{2+}, Mg^{2+}, Cu^{2+}, Cl^-, F^-, Br^-, I^-, NO_3^-, NO_2^-, N_3^-, HS^-, SO_4^{2-}, $S_2O_3^{2-}$, CN^-, AcO^-, H_2O_2, ClO^-, (10 equiv. for each); Cys (1 mM), Hcy (1 mM); GSH (5 mM). (b) Fluorescence spectra of **Mito-HN** (10 μM) in the presence of various species, including SO_3^{2-}, Ca^{2+}, Al^{3+}, Zn^{2+}, Mg^{2+}, Cu^{2+}, Cl^-, F^-, Br^-, I^-, NO_3^-, NO_2^-, N_3^-, HS^-, SO_4^{2-}, $S_2O_3^{2-}$, CN^-, AcO^-, H_2O_2, ClO^-, (10 equiv. for each); Cys (1 mM), Hcy (1 mM); GSH (5 mM).

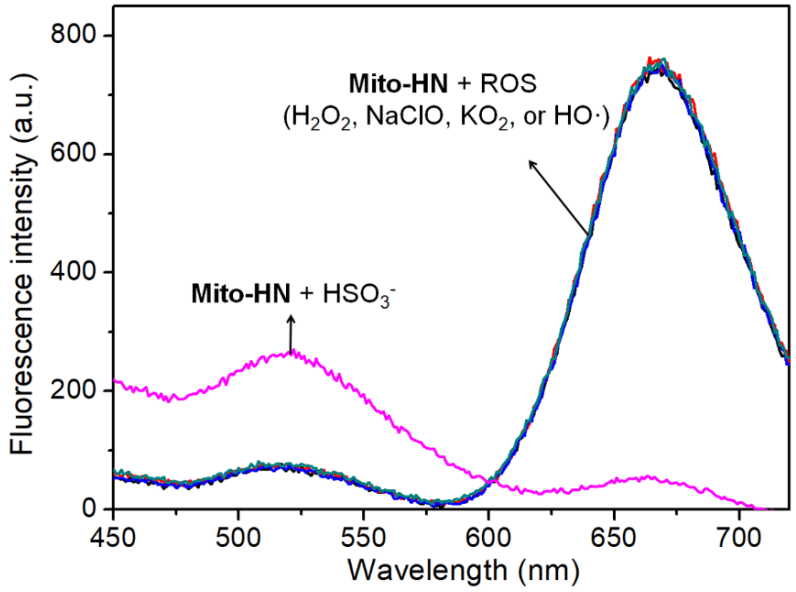

Figure S12. Fluorescence spectra of **Mito-HN** (10 μM) in the presence of reactive oxygen species (NaClO, KO_2, H_2O_2, HO·) or HSO_3^- in PBS (10 mM, pH 7.4, containing 10% DMSO).

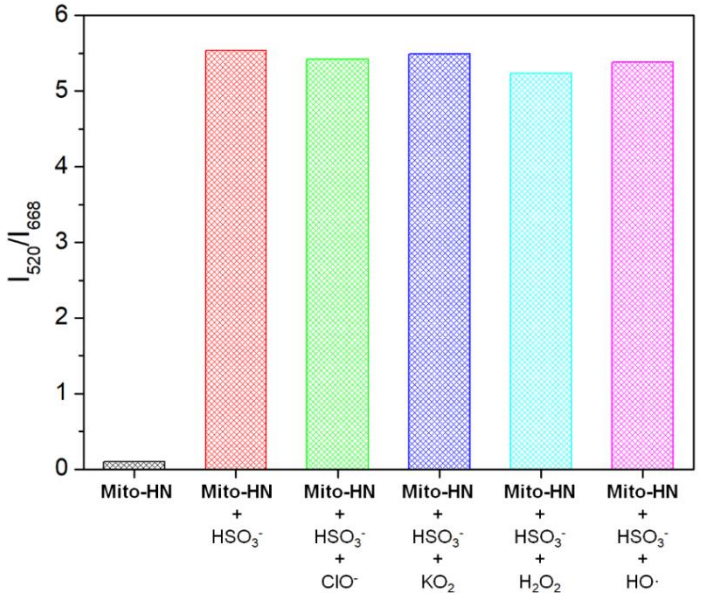

Figure S13. Fluorescence responses of **Mito-HN** (10 μM) in the presence of HSO_3^-, followed by adding reactive oxygen species (NaClO, KO_2, H_2O_2, HO·) in PBS (10 mM, pH 7.4, containing 10% DMSO).

5. CCK-8 assay.

HepG2 cells were obtained from the Chinese Academy of Sciences (Shanghai, China) and routinely cultured with Dulbecco's modified Eagle's medium supplemented with 10% fetal bovine serum, 100 U/mL penicillin, and 100 μg/mL streptomycin at 37°C in 5% CO_2 atmosphere. The cytotoxicity of **Mito-HN** to HepG2 cells was determined using **CCK-8** assay. Briefly, HepG2 cells were seeded in 96-well plates at a cell density of 5×10^4 cells/mL (200 μL/well). After 24 h incubation, cells were treated with different concentrations of **Mito-HN** (0, 2.5, 5, 10, 20, and 40 μM) and continuously incubated at 37 °C for 24 h. After washing with PBS, cells were further cultured by both CCK-8 solution (10 μL/well) and supplemented cell culture medium (190 μL/well) for 2 h. The absorbance was measured using a microplate spectrophotometer at 450 nm. Each experiment was repeated at least five times. Blank controls were run simultaneously during each experiment. As shown in Figure S10, the percentage of viable HepG2 cells after treatment with 0 - 40 μM of **Mito-HN** for 24 h was over 80%, which demonstrated that probe **Mito-HN** exhibited low cytotoxicity.

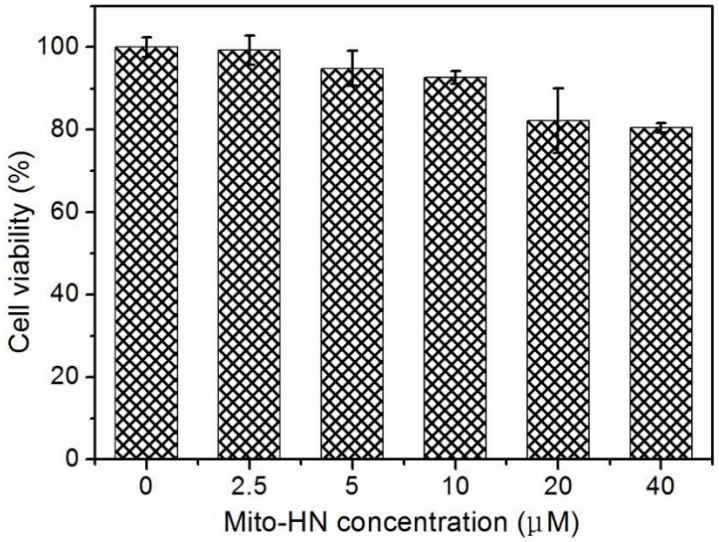

Figure S14. Cytotoxicity assay of **Mito-HN** for HepG2 cell after 24-h culture.

6. Cell imaging

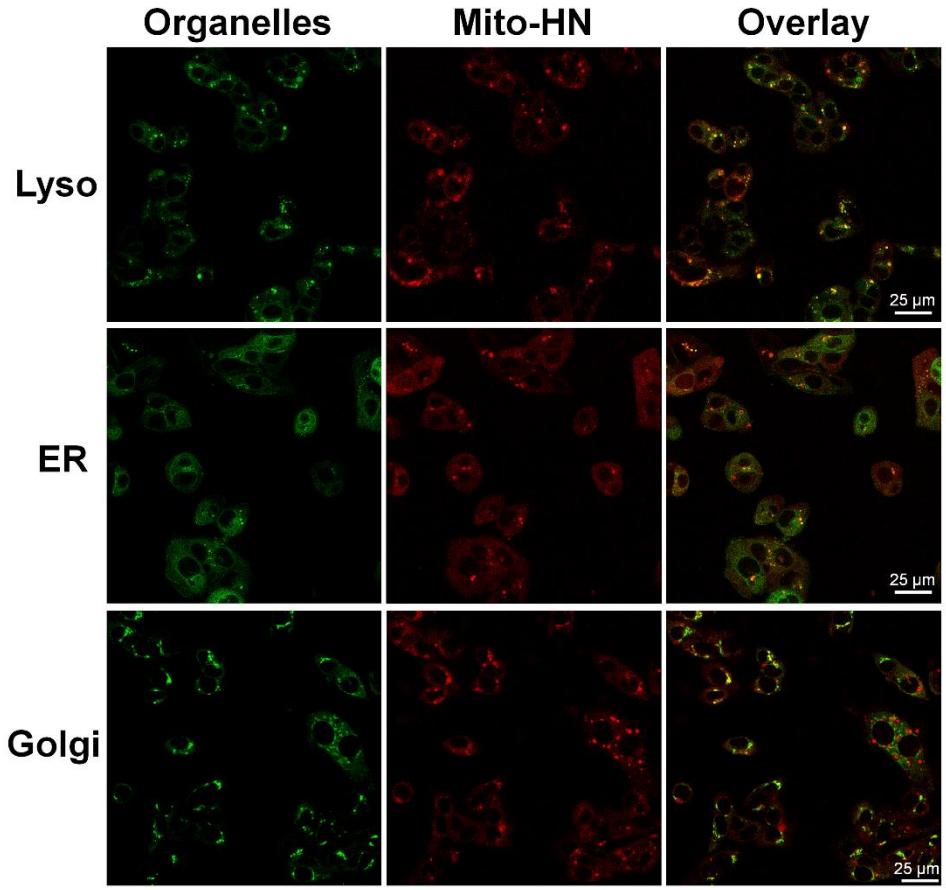

Figure S15. Colocalization fluorescence images of HepG2 cells stained with **Mito-HN** and organelles dyes. The first column: fluorescence images from Lyso-Tracker Green (1 μM, Ex = 488 nm, collected 500-570 nm), ER-Tracker Green (1 μM, Ex = 488 nm, collected 500-570 nm), Golgi-Tracker Green (1 μM, Ex=488 nm, collected 500-570 nm); The second column: fluorescence images from **Mito-HN** (10 μM, Ex= 405 nm, collected 600-700 nm); The third column: overlay images. The colocalization coefficient was about 0.35, 0.33, 0.41 for lysosomes, endoplasmic reticulum, Golgi apparatus, respectively.

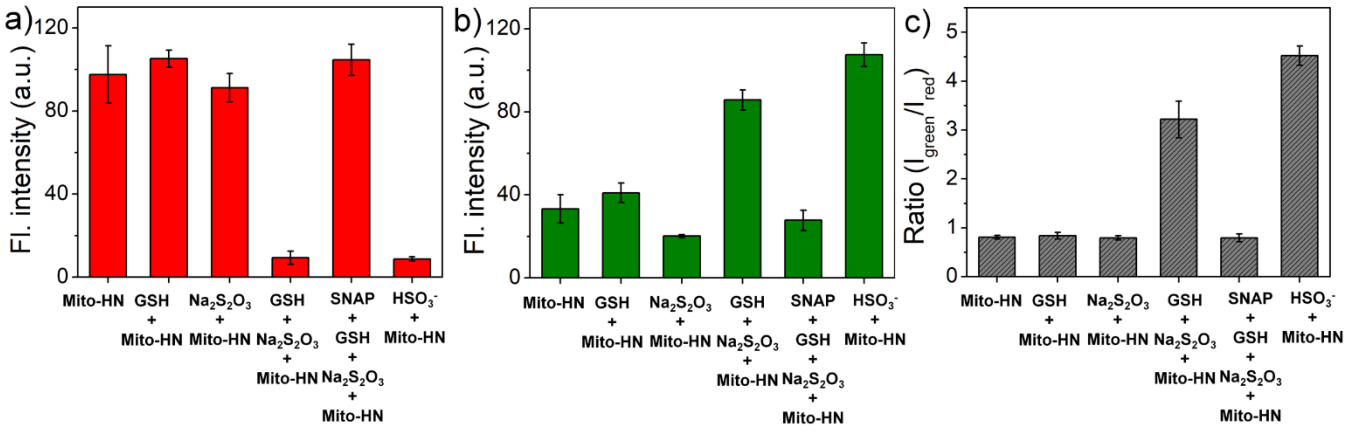

Figure S16. The quantification analyses of red, green, and ratiometric signals in living cell imaging in Figure 4.

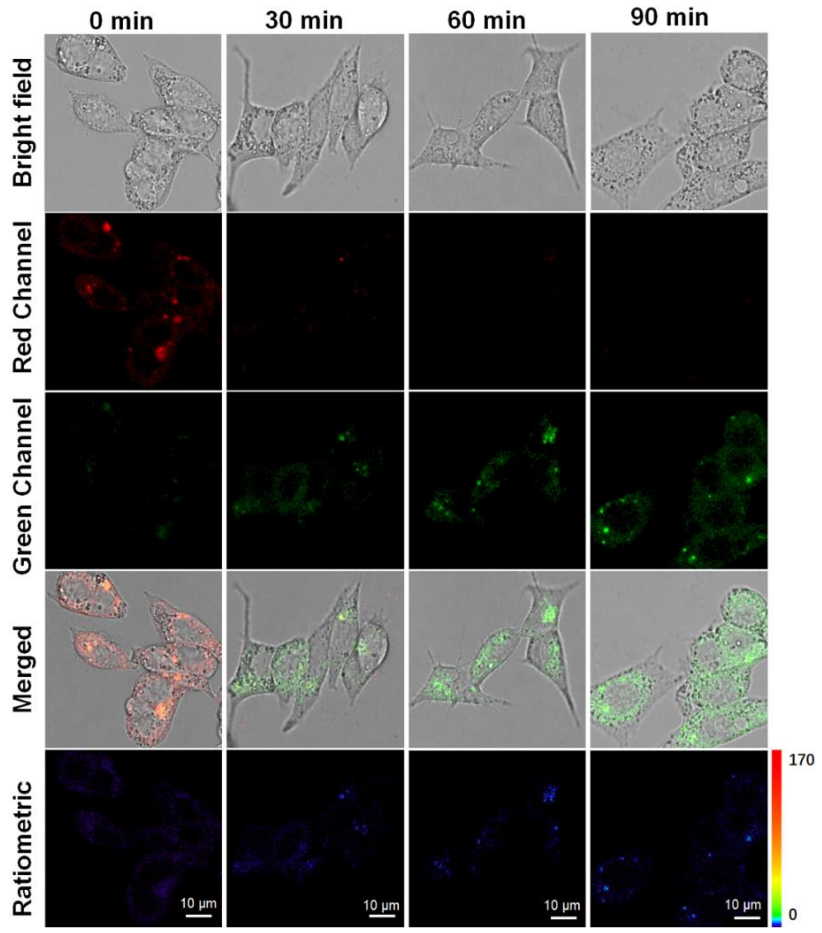

Figure S17. Fluorescence images of **Mito-HN** responding to HSO_3^- in HepG2 cells. From left to right: HepG2 cells pretreated with **Mito-HN** (10 μM) for 30 min, incubated with 100 μM $NaHSO_3$ for 0, 30, 60, 90 min, and then imaged. From up to down: Bright field; Red channel (λ_{em} = 600-700 nm); Green channel (λ_{em} = 470-560 nm); Merge; Ratiometric images (I_{green}/I_{red}).

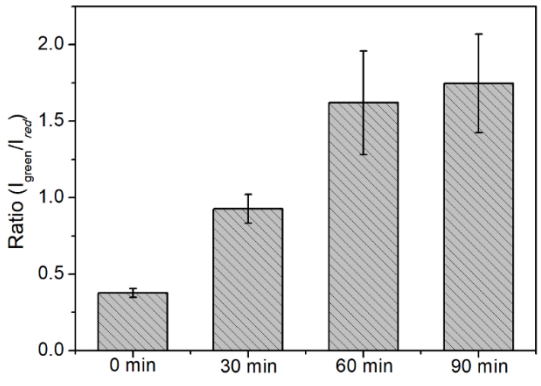

Figure S18. The quantification analyses of ratiometric signals in Figure S17.

7. References.

S1. Wang, J.; Hao, Y.; Wang, H.; Yang, S.; Tian, H.; Sun, B.; Liu, Y. Rapidly responsive and highly selective fluorescent probe for bisulfite detection in food. *J. Agric. Food Chem.* **2017**, *65*, 2883-2887.

S2. Sun, Y.; Liu, J.; Zhang, J.; Yang, T.; Guo, W. Fluorescent probe for biological gas SO_2 derivatives bisulfite and sulfite. *Chem. Commun.* **2013**, *49*, 2637−2639.

S3. Zhang, W.; Huo, F.; Zhang, Y.; Yin, C. Dual-site functionalized NIR fluorescent material for a discriminative concentration-dependent response to SO_2 in cells and mice. *J. Mater. Chem. B* **2019**, *7*, 1945-1950.